2021 American Control Conference (ACC)
New Orleans, USA, May 25-28, 2021

Optimal Actuator/Sensor Precision for Covariance Steering with Soft Convex Constraints on State and Control

Raman Goyal[1], Manoranjan Majji[2], and Robert E. Skelton[3]

***Abstract*— This paper provides the design strategy to calculate optimal precision for sensors and actuators during the covariance steering of a linear time-varying system. The covariance steering problem involves steering the statistics of the state from a known mean and covariance to the desired mean and covariance while minimizing a given cost function. A budget constraint is also considered for the design with the price values of the actuator and sensors assumed to be proportional to their precision values. The solution to the problem is given in the form of Linear Matrix Inequalities (LMIs) proving it to be a convex problem. Soft convex constraints on state and input variables are also considered in the formulation. Optimal affine output feedback control gains and optimal precision of sensors and actuators are simultaneously calculated for a soft spacecraft landing problem as an example.**

I. Introduction

In the control problems, traditionally, the control system is designed to achieve the desired performance for a given set of actuators and sensors with their pre-specified precision values. However, it is well understood now that the design of the controller and design of architecture are not two independent problems and should be integrated to meet performance objectives [1], [2]. Researchers in the past chose the sets of actuators and sensors to increase the controllability and observability of the system, however increasing the controllability/observability of the system does not necessarily result in an improved performance [3]–[5]. Li *et al.* [6] was the first one to provide the formulation to design a controller and simultaneously select the actuator and sensor precisions to bound the steady-state output covariance for a linear time-invariant system. This work provides the formulation to design an affine output feedback controller and precision architecture for the sensor/actuators to meet the performance objectives of a finite-horizon covariance steering problem for a discrete-time linear time-varying system. It is also shown that the integration of information architecture and control design is a convex problem for the desired constraints of meeting the mean and covariance requirements at the final time while minimizing a quadratic cost function.

The "Covariance Assignment" problem has been an active area of research since the 1980s with most of the research done on bounding the steady-state covariance for output and states for both continuous and discrete-time systems [7]–[9]. Recently, Chen *et al.* [10]–[12] first studied the finite-horizon steering of covariance from known Gaussian distribution to desired Gaussian distribution for continuous-time systems relating it to the optimal mass transfer problem. Since then, there has been an increasing interest in the finite-horizon covariance steering of linear systems with different types of constraints [13]–[15]. These finite-horizon steering problems have shown to be convex, thus allowing for a very fast and reliable solution. The increasing interest can be attributed to its use in applications like vehicle path planning with convex and non-convex state constraints [16], where non-convex path constraints are handled by dividing the path into an admissible set of convex sets and by choosing one of the convex set using mixed-integer convex programming. The constraints used in the paper are chance constraints which are formulated to satisfy the constraints with pre-specified (high) probability [17]. Researchers have also used the covariance steering approach to solve the power descent guidance algorithm in the presence of random noise [18]. A solution for the nonlinear dynamical system was also recently proposed as an iterative covariance steering with convex state chance constraints [19].

This paper builds on the foundation of the above-mentioned research and allows for further addition of optimum information architecture with control design to solve the covariance steering problem as a convex programming problem. The formulation of this paper is as follows: system definition and required mathematical preliminaries are provided in Section II along with the notations used in the paper. The sensors and actuators are assumed to generate i.i.d noise with their precision defined as the inverse of the respective variances. Section III formulates the problem statement

[1]TEES Postdoctoral Researcher, Department of Aerospace Engineering, Texas A&M University, College Station, TX 77840. Email: *ramaniitrgoyal92@tamu.edu*

[2]Assistant Professor, Department of Aerospace Engineering, Texas A&M University, College Station, TX 77840. Email: *mmajji@tamu.edu*

[3]TEES Distinguished Research Professor, Department of Aerospace Engineering, Texas A&M University, College Station, TX 77840. Email: *bobskelton@tamu.edu*

978-1-6654-4197-1/$31.00 ©2021 AACC

and provides the solution for the simultaneous design of information architecture and an affine output feedback controller to steer the covariance from the known distribution to a desired mean and covariance while minimizing the expected value of the quadratic cost that depends on the state and control. The solution to this problem is shown to be convex with constraints formulated as LMIs and cost as affine function. Section IV and Section V allow for the addition of soft convex constraints on the state and control input as additional LMIs. The soft landing of the spacecraft is simulated as an example to show the efficacy of the formulation in Section VI.

II. Problem Formulation

A. Notation

The set of n-dimensional real vectors are denoted by $\mathbb{R}^n$. The matrices are defined by bold uppercase letters as $\boldsymbol{Y}$. The expectation operator is defined by $\mathbb{E}[\cdot]$ and $\mathcal{N}(x, \boldsymbol{Y})$ denotes the Gaussian distribution with mean x and covariance $\boldsymbol{Y}$. The transpose of a matrix $\boldsymbol{Y}$ is defined by $\boldsymbol{Y}^T$, the diagonal matrix generated from a vector x is denoted as $\mathbf{diag}(x)$ and the block diagonal matrix is denoted as $\mathbf{blkdiag}(\boldsymbol{Y}_1, \boldsymbol{Y}_2, \cdots, \boldsymbol{Y}_3)$. The symbol $\mathbf{0}$ defines a zero matrix with suitable dimensions. The notations $\boldsymbol{X} \succ 0$ and $\boldsymbol{Y} \succeq 0$ denote the symmetric positive definite ($\mathbb{S}_n^{++}$) and symmetric positive semidefinite ($\mathbb{S}_n^{+}$) matrices, respectively.

B. System Definition

A discrete-time linear time-varying system is described by the following state-space representation:

$$x_{k+1} = \boldsymbol{A}_k x_k + \boldsymbol{B}_k u_k + \boldsymbol{D}_k w_k + \boldsymbol{E}_k w_k^a, \quad (1)$$
$$y_k = \boldsymbol{C}_k x_k + \boldsymbol{F}_k w_k^s, \quad (2)$$

for $k = \{0, 1, \cdots, N\}$ and where $x_k \in \mathbb{R}^n$ is the state of the system at time-step k, $u_k \in \mathbb{R}^m$ is the control vector, $y_k \in \mathbb{R}^p$ is the output of the system. The noise in the system is added through process noise w_k, actuator noise w_k^a and sensor noise w_k^s. These noisy inputs to the system are modeled as independent zero mean white noises with covariances $\mathbb{W} \succ 0$, $\mathbb{W}^a \succ 0$ and $\mathbb{W}^s \succ 0$, respectively, i.e.:

$$\mathbb{E}[w] = \mathbf{0}, \ \mathbb{E}[w^a] = \mathbf{0}, \ \mathbb{E}[w^s] = \mathbf{0}, \quad (3)$$
$$\mathbb{E}[ww^T] = \mathbb{W}, \ \mathbb{E}[w^a w^{a^T}] = \mathbb{W}^a, \ \mathbb{E}[w^s w^{s^T}] = \mathbb{W}^s, \quad (4)$$

where $\mathbb{E}[x]$ denotes the expected value of the random variable x. We assume the process noise covariance $\mathbb{W}$ to be known and fixed. The actuators and sensors are assumed to be independent of each other and their precisions are defined to be inversely proportional to the respective noise covariances.

$$\boldsymbol{\Gamma}^a \triangleq \mathbb{W}^{a^{-1}}, \quad \boldsymbol{\Gamma}^s \triangleq \mathbb{W}^{s^{-1}}. \quad (5)$$

We also define the vectors γ_a and γ_s such that:

$$\boldsymbol{\Gamma}^a \triangleq \mathbf{diag}(\gamma_a), \quad \boldsymbol{\Gamma}^s \triangleq \mathbf{diag}(\gamma_s). \quad (6)$$

Similar to [6], we associate a price to each actuator/sensor that is inversely proportional to the noise intensity associated with that instrument. Therefore, the total design price can be expressed as:

$$\$ = p_a^T \gamma_a + p_s^T \gamma_s, \quad (7)$$

where p_a and p_s are vectors containing the price per unit of actuator precision and sensor precision, respectively.

C. Mathematical Preliminaries

In this subsection, we discuss the preliminary mathematical formulation needed for the important results in the next section. Let us define the system matrices as:

$$\boldsymbol{A}_{k_1,k_0} \triangleq \boldsymbol{A}_{k_1} \boldsymbol{A}_{k_1-1} \cdots \boldsymbol{A}_{k_0}, \quad (8)$$
$$\boldsymbol{B}_{k_1,k_0} \triangleq \boldsymbol{A}_{k_1,k_0+1} \boldsymbol{B}_{k_0}, \quad (9)$$
$$\boldsymbol{D}_{k_1,k_0} \triangleq \boldsymbol{A}_{k_1,k_0+1} \boldsymbol{D}_{k_0}, \ \boldsymbol{E}_{k_1,k_0} \triangleq \boldsymbol{A}_{k_1,k_0+1} \boldsymbol{E}_{k_0}, \quad (10)$$

and let us also define the following matrices as:

$$\bar{\boldsymbol{A}}_k \triangleq \boldsymbol{A}_{k,0}, \ \bar{\boldsymbol{B}}_k \triangleq [\boldsymbol{B}_{k,0} \ \boldsymbol{B}_{k,1} \ \cdots \ \boldsymbol{B}_k], \quad (11)$$
$$\bar{\boldsymbol{D}}_k \triangleq [\boldsymbol{D}_{k,0} \ \boldsymbol{D}_{k,1} \ \cdots \ \boldsymbol{D}_k], \ \bar{\boldsymbol{E}}_k \triangleq [\boldsymbol{E}_{k,0} \ \boldsymbol{E}_{k,1} \ \cdots \ \boldsymbol{E}_k]. \quad (12)$$

Using the above mentioned definitions, the system dynamics eq. (1) can be written as:

$$x_{k+1} = \bar{\boldsymbol{A}}_k x_0 + \bar{\boldsymbol{B}}_k U_k + \bar{\boldsymbol{D}}_k W_k + \bar{\boldsymbol{E}}_k W_k^a, \quad (13)$$

where the vectors U_k, W_k and W_k^a are defined as:

$$U_k = \begin{bmatrix} u_0 \\ u_1 \\ \vdots \\ u_k \end{bmatrix}, \ W_k = \begin{bmatrix} w_0 \\ w_1 \\ \vdots \\ w_k \end{bmatrix}, \ W_k^a = \begin{bmatrix} w_0^a \\ w_1^a \\ \vdots \\ w_k^a \end{bmatrix}, \quad (14)$$

and the output equation at time k can be written as:

$$y_k = \boldsymbol{C}_k \bar{\boldsymbol{A}}_{k-1} x_0 + \boldsymbol{C}_k \bar{\boldsymbol{B}}_{k-1} U_{k-1} + \boldsymbol{C}_k \bar{\boldsymbol{D}}_{k-1} W_{k-1} + \boldsymbol{C}_k \bar{\boldsymbol{E}}_{k-1} W_{k-1}^a + \boldsymbol{F}_k w_k^s. \quad (15)$$

Let us write the state equation in augmented vector form as:

$$X_{k+1} = \boldsymbol{\mathcal{A}}_k x_0 + \boldsymbol{\mathcal{B}}_k U_k + \boldsymbol{\mathcal{D}}_k W_k + \boldsymbol{\mathcal{E}}_k W_k^a, \quad (16)$$

where

$$X_{k+1} = \begin{bmatrix} x_0 \\ x_1 \\ \vdots \\ x_{k+1} \end{bmatrix}, \ \boldsymbol{\mathcal{A}}_k = \begin{bmatrix} I \\ \bar{\boldsymbol{A}}_0 \\ \vdots \\ \bar{\boldsymbol{A}}_k \end{bmatrix}, \tag{17}$$

$$\boldsymbol{\mathcal{B}}_k = \begin{bmatrix} \mathbf{0} & \mathbf{0} \\ \bar{\boldsymbol{B}}_0 & \mathbf{0} \\ \bar{\boldsymbol{B}}_1 & \mathbf{0} \\ \vdots & \\ \bar{\boldsymbol{B}}_k & \mathbf{0} \end{bmatrix}, \ \boldsymbol{\mathcal{D}}_k = \begin{bmatrix} \mathbf{0} & \mathbf{0} \\ \bar{\boldsymbol{D}}_0 & \mathbf{0} \\ \bar{\boldsymbol{D}}_1 & \mathbf{0} \\ \vdots & \\ \bar{\boldsymbol{D}}_k & \mathbf{0} \end{bmatrix}, \ \boldsymbol{\mathcal{E}}_k = \begin{bmatrix} \mathbf{0} & \mathbf{0} \\ \bar{\boldsymbol{E}}_0 & \mathbf{0} \\ \bar{\boldsymbol{E}}_1 & \mathbf{0} \\ \vdots & \\ \bar{\boldsymbol{E}}_k & \mathbf{0} \end{bmatrix}. \tag{18}$$

Let us write the output equation in augmented vector form as:

$$Y_k = \boldsymbol{\mathcal{C}}_k X_k + \boldsymbol{\mathcal{F}}_k W_k^s, \tag{19}$$

where

$$\boldsymbol{\mathcal{C}}_k = \textbf{blkdiag}(\boldsymbol{C}_0, \boldsymbol{C}_1, \cdots, \boldsymbol{C}_k), \tag{20}$$

$$\boldsymbol{\mathcal{F}}_k = \textbf{blkdiag}(\boldsymbol{F}_0, \boldsymbol{F}_1, \cdots, \boldsymbol{F}_k), \tag{21}$$

and

$$Y_k = \begin{bmatrix} y_0 & y_1 & \cdots & y_k \end{bmatrix}^T, \tag{22}$$

$$W_k^s = \begin{bmatrix} w_0^s & w_1^s & \cdots & w_k^s \end{bmatrix}^T, \tag{23}$$

which can further be written after substitution as:

$$\begin{aligned} Y_k = \boldsymbol{\mathcal{C}}_k \boldsymbol{\mathcal{A}}_{k-1} x_0 + \boldsymbol{\mathcal{C}}_k \boldsymbol{\mathcal{B}}_{k-1} U_{k-1} + \boldsymbol{\mathcal{C}}_k \boldsymbol{\mathcal{D}}_{k-1} W_{k-1} \\ + \boldsymbol{\mathcal{C}}_k \boldsymbol{\mathcal{E}}_{k-1} W_{k-1}^a + \boldsymbol{\mathcal{F}}_k W_k^s. \end{aligned} \tag{24}$$

The next section will make use of the augmented state equation (eq. (16)) and augmented output equation (eq. (24)) to solve the optimal precision allocation for the covariance steering problem.

III. Optimal Architecture for the Covariance Steering Problem

A. Problem Statement

In this work, we consider an affine feedback law comprising of two parts: a feedforward control vector V_N and a feedback gain matrix $\bar{\boldsymbol{K}}_N$ (similar to optimal covariance steering solution [16]). So, the final problem statement is to find the control law (V_N, $\bar{\boldsymbol{K}}_N$) and simultaneously select the appropriate actuator and sensor precisions such that the statistics of the state can be steered from:

$$x_0 \sim \mathcal{N}(\mu_0, \boldsymbol{\Sigma}_0) \text{ to } x_{N+1} \sim \mathcal{N}(\mu_{N+1}, \boldsymbol{\Sigma}_{N+1}), \tag{25}$$

while minimizing the cost function J:

$$J = \mathbb{E}\left[\sum_{k=0}^{N} \left((x_k - \mu_{N+1})^T \boldsymbol{Q}_k (x_k - \mu_{N+1}) + u_k^T \boldsymbol{R}_k u_k\right)\right], \tag{26}$$

with the budget and precisions constraints as:

$$\$ < \bar{\$}, \quad \gamma_a < \bar{\gamma}_a, \quad \gamma_s < \bar{\gamma}_s, \tag{27}$$

for given $\bar{\$} > 0$, $\bar{\gamma}_a > \mathbf{0}$, $\bar{\gamma}_s > \mathbf{0}$, μ_0, μ_{N+1}, $\boldsymbol{\Sigma}_0 \succ 0$ and $\boldsymbol{\Sigma}_{N+1} \succeq 0$. The bounds on precision values can be added based on the most precise sensor available in the market. The constraint on mean and covariance at final time can be written as:

$$\mathbb{E}[x_{N+1}] = \mu_{N+1}, \quad \mathbb{E}[\tilde{x}_{N+1}\tilde{x}_{N+1}^T] \preceq \boldsymbol{\Sigma}_{N+1}, \tag{28}$$

where a bound is put on the covariance instead of exactly matching it [8].

B. Solution to the Problem Statement

Theorem 3.1: Let a discrete-time time-varying linear system be described by the state space equation (1) and the output equation (2). The feedforward control vector V_N, the feedback control matrix $\bar{\boldsymbol{K}}_N$ for the output-feedback controller and vectors of actuator and sensor precision γ_a, γ_s, that minimize the cost function (eq. (26)) and satisfy the constraints (eqs. (27) and (28)), can be solved using the following linear matrix equalities and inequalities:

$$\min. \ (\text{Tr}(\boldsymbol{J}_x) + \text{Tr}(\boldsymbol{J}_u)) \tag{29}$$

such that

$$p_a^T \gamma_a + p_s^T \gamma_s < \bar{\$}, \tag{30}$$

$$\gamma_a < \bar{\gamma}_a, \quad \gamma_s < \bar{\gamma}_s, \tag{31}$$

$$\boldsymbol{\mathcal{I}}_N(\boldsymbol{\mathcal{A}}_N \mu_0 + \boldsymbol{\mathcal{B}}_N V_N) = \mu_{N+1}, \tag{32}$$

$$\begin{bmatrix} \boldsymbol{\Sigma}_{N+1} & \boldsymbol{\mathcal{I}}_N \boldsymbol{\mathcal{G}}_1 & \boldsymbol{\mathcal{I}}_N \boldsymbol{\mathcal{G}}_2 & \boldsymbol{\mathcal{I}}_N \boldsymbol{\mathcal{G}}_3 & \boldsymbol{\mathcal{I}}_N \boldsymbol{\mathcal{G}}_4 \\ (\bullet_{12})^T & \boldsymbol{\Sigma}_0^{-1} & \mathbf{0} & \mathbf{0} & \mathbf{0} \\ (\bullet_{13})^T & \mathbf{0} & \mathbb{W}_N^{-1} & \mathbf{0} & \mathbf{0} \\ (\bullet_{14})^T & \mathbf{0} & \mathbf{0} & \boldsymbol{\Gamma}_N^a & \mathbf{0} \\ (\bullet_{15})^T & \mathbf{0} & \mathbf{0} & \mathbf{0} & \boldsymbol{\Gamma}_N^s \end{bmatrix} \succeq \mathbf{0}, \tag{33}$$

$$\begin{bmatrix} \boldsymbol{J}_x & (\star) & \bar{\boldsymbol{Q}}^{\frac{1}{2}} \boldsymbol{\mathcal{G}}_1 & \bar{\boldsymbol{Q}}^{\frac{1}{2}} \boldsymbol{\mathcal{G}}_2 & \bar{\boldsymbol{Q}}^{\frac{1}{2}} \boldsymbol{\mathcal{G}}_3 & \bar{\boldsymbol{Q}}^{\frac{1}{2}} \boldsymbol{\mathcal{G}}_4 \\ (\bullet_{12})^T & \boldsymbol{I} & \mathbf{0} & \mathbf{0} & \mathbf{0} & \mathbf{0} \\ (\bullet_{13})^T & \mathbf{0} & \boldsymbol{\Sigma}_0^{-1} & \mathbf{0} & \mathbf{0} & \mathbf{0} \\ (\bullet_{14})^T & \mathbf{0} & \mathbf{0} & \mathbb{W}_N^{-1} & \mathbf{0} & \mathbf{0} \\ (\bullet_{15})^T & \mathbf{0} & \mathbf{0} & \mathbf{0} & \boldsymbol{\Gamma}_N^a & \mathbf{0} \\ (\bullet_{16})^T & \mathbf{0} & \mathbf{0} & \mathbf{0} & \mathbf{0} & \boldsymbol{\Gamma}_N^s \end{bmatrix} \succeq \mathbf{0}, \tag{34}$$

where

$$(\star) = \bar{\boldsymbol{Q}}^{\frac{1}{2}}(\boldsymbol{\mathcal{A}}_N \mu_0 + \boldsymbol{\mathcal{B}}_N V_N - \bar{\mu}_{N+1}),$$

$$\boldsymbol{\mathcal{G}}_1 = (\boldsymbol{I} + \boldsymbol{\mathcal{B}}_N \boldsymbol{\mathcal{K}}_N \boldsymbol{\mathcal{C}}_{N+1}) \boldsymbol{\mathcal{A}}_N,$$

$$\boldsymbol{\mathcal{G}}_2 = (\boldsymbol{I} + \boldsymbol{\mathcal{B}}_N \boldsymbol{\mathcal{K}}_N \boldsymbol{\mathcal{C}}_{N+1}) \boldsymbol{\mathcal{D}}_N,$$

$$\boldsymbol{\mathcal{G}}_3 = (\boldsymbol{I} + \boldsymbol{\mathcal{B}}_N \boldsymbol{\mathcal{K}}_N \boldsymbol{\mathcal{C}}_{N+1}) \boldsymbol{\mathcal{E}}_N, \ \boldsymbol{\mathcal{G}}_4 = \boldsymbol{\mathcal{B}}_N \boldsymbol{\mathcal{K}}_N \boldsymbol{\mathcal{F}}_{N+1},$$

$$\mathbb{W}_N = \boldsymbol{I}_N \otimes \mathbb{W}, \ \boldsymbol{\Gamma}_N^a = \boldsymbol{I}_N \otimes \boldsymbol{\Gamma}^a, \ \boldsymbol{\Gamma}_N^s = \boldsymbol{I}_N \otimes \boldsymbol{\Gamma}^s,$$

$$\begin{bmatrix} \boldsymbol{J}_u & \bar{\boldsymbol{R}}^{\frac{1}{2}}V_N & \bar{\boldsymbol{R}}^{\frac{1}{2}}\boldsymbol{\mathcal{H}}_1 & \bar{\boldsymbol{R}}^{\frac{1}{2}}\boldsymbol{\mathcal{H}}_2 & \bar{\boldsymbol{R}}^{\frac{1}{2}}\boldsymbol{\mathcal{H}}_3 & \bar{\boldsymbol{R}}^{\frac{1}{2}}\boldsymbol{\mathcal{H}}_4 \\ (\bullet_{12})^T & \boldsymbol{I} & \mathbf{0} & \mathbf{0} & \mathbf{0} & \mathbf{0} \\ (\bullet_{13})^T & \mathbf{0} & \boldsymbol{\Sigma}_0^{-1} & \mathbf{0} & \mathbf{0} & \mathbf{0} \\ (\bullet_{14})^T & \mathbf{0} & \mathbf{0} & \mathbb{W}_N^{-1} & \mathbf{0} & \mathbf{0} \\ (\bullet_{15})^T & \mathbf{0} & \mathbf{0} & \mathbf{0} & \boldsymbol{\Gamma}_N^a & \mathbf{0} \\ (\bullet_{16})^T & \mathbf{0} & \mathbf{0} & \mathbf{0} & \mathbf{0} & \boldsymbol{\Gamma}_N^s \end{bmatrix} \succeq \mathbf{0}, \tag{35}$$

where

$$\boldsymbol{\mathcal{H}}_1 = \boldsymbol{\mathcal{K}}_N \boldsymbol{\mathcal{C}}_{N+1} \boldsymbol{\mathcal{A}}_N, \ \boldsymbol{\mathcal{H}}_2 = \boldsymbol{\mathcal{K}}_N \boldsymbol{\mathcal{C}}_{N+1} \boldsymbol{\mathcal{D}}_N,$$
$$\boldsymbol{\mathcal{H}}_3 = \boldsymbol{\mathcal{K}}_N \boldsymbol{\mathcal{C}}_{N+1} \boldsymbol{\mathcal{E}}_N, \ \boldsymbol{\mathcal{H}}_4 = \boldsymbol{\mathcal{K}}_N \boldsymbol{\mathcal{F}}_{N+1},$$
$$\boldsymbol{\mathcal{K}}_N = [\bar{\boldsymbol{K}}_N \ \ \mathbf{0}], \ \boldsymbol{\mathcal{I}}_N = \begin{bmatrix} \mathbf{0} & \mathbf{0} & \cdots & \mathbf{0} & \boldsymbol{I}_n \end{bmatrix},$$

$\boldsymbol{I}_n$ is a $n \times n$ identity matrix, $\boldsymbol{J}_x$ and $\boldsymbol{J}_u$ are two dummy matrices and $(\bullet_{ij})$ denotes the $\{ij\}^{\text{th}}$ element of that matrix.

Proof: We choose an affine control law of the following form:

$$u_k = v_k + \sum_{i=1}^{k} \left[\boldsymbol{K}_i (y_i - \boldsymbol{C}_i \bar{\boldsymbol{A}}_{i-1} \mu_0 - \boldsymbol{C}_i \bar{\boldsymbol{B}}_{i-1} U_{i-1}) \right], \tag{36}$$

which is similar to the one used in [16] and uses the output information from the system until time-step k and control input until time $k-1$ to generate the control input u_k. Let us write the control law in the augmented states as:

$$U_k = V_k + \bar{\boldsymbol{K}}_k (Y_k - \boldsymbol{\mathcal{C}}_k \boldsymbol{\mathcal{A}}_{k-1} \mu_0 - \boldsymbol{\mathcal{C}}_k \boldsymbol{\mathcal{B}}_{k-1} U_{k-1}), \tag{37}$$

where V_k is the vector generated from v_k and the left lower triangular matrix $\bar{\boldsymbol{K}}_k$ is created using $\boldsymbol{K}_i$. The control law can again be written using eq. (24) as:

$$\begin{aligned} U_k &= V_k + \bar{\boldsymbol{K}}_k \left(\boldsymbol{\mathcal{C}}_k \boldsymbol{\mathcal{A}}_{k-1} (x_0 - \mu_0) \right) \\ &+ \bar{\boldsymbol{K}}_k \left(\boldsymbol{\mathcal{C}}_k \boldsymbol{\mathcal{D}}_{k-1} W_{k-1} + \boldsymbol{\mathcal{C}}_k \boldsymbol{\mathcal{E}}_{k-1} W_{k-1}^a + \boldsymbol{\mathcal{F}}_k W_k^s \right). \end{aligned} \tag{38}$$

Let us write the control in a slightly different form by defining $\boldsymbol{\mathcal{K}}_k = [\bar{\boldsymbol{K}}_k \ \mathbf{0}]$ as:

$$\begin{aligned} U_k &= V_k + \boldsymbol{\mathcal{K}}_k \left(\boldsymbol{\mathcal{C}}_{k+1} \boldsymbol{\mathcal{A}}_k (x_0 - \mu_0) \right) \\ &+ \boldsymbol{\mathcal{K}}_k \left(\boldsymbol{\mathcal{C}}_{k+1} \boldsymbol{\mathcal{D}}_k W_k + \boldsymbol{\mathcal{C}}_{k+1} \boldsymbol{\mathcal{E}}_k W_k^a + \boldsymbol{\mathcal{F}}_{k+1} W_{k+1}^s \right). \end{aligned} \tag{39}$$

Using the control mentioned in eq. (39), we can write the state equation (eq. (16)) as:

$$\begin{aligned} X_{k+1} &= \boldsymbol{\mathcal{A}}_k x_0 + \boldsymbol{\mathcal{B}}_k V_k + \boldsymbol{\mathcal{D}}_k W_k + \boldsymbol{\mathcal{E}}_k W_k^a \\ &+ \boldsymbol{\mathcal{B}}_k \boldsymbol{\mathcal{K}}_k \boldsymbol{\mathcal{C}}_{k+1} \left(\boldsymbol{\mathcal{A}}_k (x_0 - \mu_0) + \boldsymbol{\mathcal{D}}_k W_k + \boldsymbol{\mathcal{E}}_k W_k^a \right) \\ &+ \boldsymbol{\mathcal{B}}_k \boldsymbol{\mathcal{K}}_k \boldsymbol{\mathcal{F}}_{k+1} W_{k+1}^s, \end{aligned} \tag{40}$$

Taking the expectation of the above equation, we get:

$$\bar{X}_{k+1} = \mathbb{E}[X_{k+1}] = \boldsymbol{\mathcal{A}}_k \mu_0 + \boldsymbol{\mathcal{B}}_k V_k, \tag{41}$$

and for the variation, $\tilde{X}_{k+1} = X_{k+1} - \bar{X}_{k+1}$, we get:

$$\begin{aligned} \tilde{X}_{k+1} &= \boldsymbol{\mathcal{A}}_k (x_0 - \mu_0) + \boldsymbol{\mathcal{D}}_k W_k + \boldsymbol{\mathcal{E}}_k W_k^a \\ &+ \boldsymbol{\mathcal{B}}_k \boldsymbol{\mathcal{K}}_k \boldsymbol{\mathcal{C}}_{k+1} \left(\boldsymbol{\mathcal{A}}_k (x_0 - \mu_0) + \boldsymbol{\mathcal{D}}_k W_k + \boldsymbol{\mathcal{E}}_k W_k^a \right) \\ &+ \boldsymbol{\mathcal{B}}_k \boldsymbol{\mathcal{K}}_k \boldsymbol{\mathcal{F}}_{k+1} W_{k+1}^s, \end{aligned} \tag{42}$$

which can again be written as:

$$\begin{aligned} \tilde{X}_{k+1} &= (I + \boldsymbol{\mathcal{B}}_k \boldsymbol{\mathcal{K}}_k \boldsymbol{\mathcal{C}}_{k+1}) \left(\boldsymbol{\mathcal{A}}_k \tilde{x}_0 + \boldsymbol{\mathcal{D}}_k W_k + \boldsymbol{\mathcal{E}}_k W_k^a \right) \\ &+ \boldsymbol{\mathcal{B}}_k \boldsymbol{\mathcal{K}}_k \boldsymbol{\mathcal{F}}_{k+1} W_{k+1}^s, \end{aligned} \tag{43}$$

where $\tilde{x}_0 = x_0 - \mu_0$ and the covariance at any time $k+1$ can be written as:

$$\begin{aligned} \mathbb{E}[\tilde{X}_{k+1} \tilde{X}_{k+1}^T] &= \boldsymbol{\mathcal{B}}_k \boldsymbol{\mathcal{K}}_k \boldsymbol{\mathcal{F}}_{k+1} \mathbb{W}_{k+1}^s (\boldsymbol{\mathcal{B}}_k \boldsymbol{\mathcal{K}}_k \boldsymbol{\mathcal{F}}_{k+1})^T \\ &+ (\boldsymbol{I} + \boldsymbol{\mathcal{B}}_k \boldsymbol{\mathcal{K}}_k \boldsymbol{\mathcal{C}}_{k+1}) \left(\boldsymbol{\mathcal{A}}_k \boldsymbol{\Sigma}_0 \boldsymbol{\mathcal{A}}_k^T \right) (\boldsymbol{I} + \boldsymbol{\mathcal{B}}_k \boldsymbol{\mathcal{K}}_k \boldsymbol{\mathcal{C}}_{k+1})^T \\ &+ (\boldsymbol{I} + \boldsymbol{\mathcal{B}}_k \boldsymbol{\mathcal{K}}_k \boldsymbol{\mathcal{C}}_{k+1}) \left(\boldsymbol{\mathcal{D}}_k \mathbb{W}_k \boldsymbol{\mathcal{D}}_k^T \right) (\boldsymbol{I} + \boldsymbol{\mathcal{B}}_k \boldsymbol{\mathcal{K}}_k \boldsymbol{\mathcal{C}}_{k+1})^T \\ &+ (\boldsymbol{I} + \boldsymbol{\mathcal{B}}_k \boldsymbol{\mathcal{K}}_k \boldsymbol{\mathcal{C}}_{k+1}) \left(\boldsymbol{\mathcal{E}}_k \mathbb{W}_k^a \boldsymbol{\mathcal{E}}_k^T \right) (\boldsymbol{I} + \boldsymbol{\mathcal{B}}_k \boldsymbol{\mathcal{K}}_k \boldsymbol{\mathcal{C}}_{k+1})^T. \end{aligned} \tag{44}$$

Finally, the mean for the final time $k = N+1$ can be written as:

$$\bar{x}_{N+1} = \boldsymbol{\mathcal{I}}_N \bar{X}_{N+1} = \boldsymbol{\mathcal{I}}_N (\boldsymbol{\mathcal{A}}_N \mu_0 + \boldsymbol{\mathcal{B}}_N V_N), \tag{45}$$

which is the constraint given in eq. (32) and the covariance at the final time can be written as:

$$\mathbb{E}[\tilde{x}_{N+1} \tilde{x}_{N+1}^T] = \boldsymbol{\mathcal{I}}_N \mathbb{E}[\tilde{X}_{N+1} \tilde{X}_{N+1}^T] \boldsymbol{\mathcal{I}}_N^T, \tag{46}$$

which should be bounded by the specified final covariance constraint:

$$\mathbb{E}[\tilde{x}_{N+1} \tilde{x}_{N+1}^T] \preceq \boldsymbol{\Sigma}_{N+1}, \tag{47}$$

which further can be written as a linear matrix inequality given in eq. (33) using the Schur's complement with the given definition of $\boldsymbol{\mathcal{G}}_i$ for $i = 1, 2, 3, 4$ and $\boldsymbol{\Gamma}_N^a = {\mathbb{W}_N^a}^{-1}$, $\boldsymbol{\Gamma}_N^s = {\mathbb{W}_N^s}^{-1}$.

Now, the cost function given in eq. (26) can be written as:

$$J = \mathbb{E}[(X_N - \bar{\mu}_{N+1})^T \bar{\boldsymbol{Q}} (X_N - \bar{\mu}_{N+1}) + U_N^T \bar{\boldsymbol{R}} U_N], \tag{48}$$

where $\bar{\boldsymbol{Q}} = \boldsymbol{I}_N \otimes \boldsymbol{Q}$, $\bar{\mu}_{N+1} = \mathbf{1}_N \otimes \mu_{N+1}$ and $\bar{\boldsymbol{R}} = \boldsymbol{I}_N \otimes \boldsymbol{R}$. The cost function can again be written as:

$$\begin{aligned} J &= (\bar{X}_N - \bar{\mu}_{N+1})^T \bar{\boldsymbol{Q}} (\bar{X}_N - \bar{\mu}_{N+1}) + \mathbb{E}[\tilde{X}_N^T \bar{\boldsymbol{Q}} \tilde{X}_N] \\ &+ V_N^T \bar{\boldsymbol{R}} V_N + \mathbb{E}[\tilde{U}_N^T \bar{\boldsymbol{R}} \tilde{U}_N], \end{aligned} \tag{49}$$

and after combining the terms and using the properties of the trace operator, we can write:

$$\begin{aligned} J &= \mathrm{Tr}(\bar{\boldsymbol{Q}} (\bar{X}_N - \bar{\mu}_{N+1})(\bar{X}_N - \bar{\mu}_{N+1})^T + \bar{\boldsymbol{Q}} \mathbb{E}[\tilde{X}_N \tilde{X}_N^T]) \\ &+ \mathrm{Tr}(\bar{\boldsymbol{R}} V_N V_N^T + \bar{\boldsymbol{R}} \mathbb{E}[\tilde{U}_N \tilde{U}_N^T]), \end{aligned} \tag{50}$$

where $\mathrm{Tr}(\cdot)$ is the trace operator. Let us write the final cost minimization as:

$$\min.\left(\mathrm{Tr}(\boldsymbol{J}_x)+\mathrm{Tr}(\boldsymbol{J}_u)\right), \tag{51}$$

where we add the constraints on dummy variables J_x and J_u as:

$$\begin{aligned}\boldsymbol{J}_x \succeq \bar{\boldsymbol{Q}}^{1/2}(\bar{X}_N-\bar{\mu}_{N+1})(\bar{X}_N-\bar{\mu}_{N+1})^T\bar{\boldsymbol{Q}}^{1/2}\\ +\bar{\boldsymbol{Q}}^{1/2}\mathbb{E}[\tilde{X}_N\tilde{X}_N^T]\bar{\boldsymbol{Q}}^{1/2},\end{aligned} \tag{52}$$

$$\boldsymbol{J}_u \succeq \bar{\boldsymbol{R}}^{1/2}V_NV_N^T\bar{\boldsymbol{R}}^{1/2}+\bar{\boldsymbol{R}}^{1/2}\mathbb{E}[\tilde{U}_N\tilde{U}_N^T]\bar{\boldsymbol{R}}^{1/2}. \tag{53}$$

The above matrix inequalities can finally be written as linear matrix inequalities (eqs. (34) and (35)) using the Schur's complement. ■

IV. Convex Constraints on the State

A lot of ground, air and space robotics motion planning applications require to steer the mean of the state with convex and non-convex constraints on the system state. In this section, we provide a methodology to add convex constraints on the state by softly incorporating the constraints of the form:

$$(x_k-\alpha_x)^T\boldsymbol{P}_x(x_k-\alpha_x)\leq\beta_x, \tag{54}$$

for $k=0,1,\cdots,N$, where α_x, $\boldsymbol{P}_x$ and β_x are parameters for convex ellipsoid which can be used to approximate problem specific design constraints. The state constraints can be forced such that the expected value of the state stays inside the defined ellipsoid:

$$\mathbb{E}[(x_k-\alpha_x)^T\boldsymbol{P}_x(x_k-\alpha_x)]\leq\beta_x, \tag{55}$$

$$(\bar{x}_k-\alpha_x)^T\boldsymbol{P}_x(\bar{x}_k-\alpha_x)+\mathbb{E}[\tilde{x}_k^T\boldsymbol{P}_x\tilde{x}_k]\leq\beta_x, \tag{56}$$

for all $k=0,1,\cdots,N$, which can again be written as:

$$\begin{aligned}(\bar{X}_N-\bar{\boldsymbol{\alpha}})^T\boldsymbol{\mathcal{I}}_k^T\boldsymbol{P}_x\boldsymbol{\mathcal{I}}_k(\bar{X}_N-\bar{\boldsymbol{\alpha}})\\ +\mathbb{E}[\tilde{X}_N^T\boldsymbol{\mathcal{I}}_k^T\boldsymbol{P}_x\boldsymbol{\mathcal{I}}_k\tilde{X}_N]\leq\beta_x,\end{aligned} \tag{57}$$

where $\bar{\boldsymbol{\alpha}}=\boldsymbol{I}_N\otimes\alpha$ and $\boldsymbol{\mathcal{I}}_k=\begin{bmatrix}\mathbf{0}\cdots\mathbf{0} & \boldsymbol{I}_k & \mathbf{0}\cdots\mathbf{0}\end{bmatrix}$ with $\boldsymbol{I}_k$ at the k^{th} place. The expected constraint on state can further be written as:

$$\begin{aligned}(\bar{X}_N-\bar{\boldsymbol{\alpha}})^T\boldsymbol{\mathcal{I}}_k^T\boldsymbol{P}_x\boldsymbol{\mathcal{I}}_k(\bar{X}_N-\bar{\boldsymbol{\alpha}})\\ +\mathrm{Tr}\left(\boldsymbol{P}_x\boldsymbol{\mathcal{I}}_k\mathbb{E}[\tilde{X}_N\tilde{X}_N^T]\boldsymbol{\mathcal{I}}_k^T\right)\leq\beta_x.\end{aligned} \tag{58}$$

Now, due to monotonicity of trace function over convex constraints, the following is true:

$$\boldsymbol{\Psi}_k^x\succeq\boldsymbol{P}_x\boldsymbol{\mathcal{I}}_k\mathbb{E}[\tilde{X}_N\tilde{X}_N^T]\boldsymbol{\mathcal{I}}_k^T, \tag{59}$$

$$\Downarrow$$

$$\mathrm{Tr}(\boldsymbol{\Psi}_k^x)\geq\mathrm{Tr}\left(\boldsymbol{P}_x\boldsymbol{\mathcal{I}}_k\mathbb{E}[\tilde{X}_N\tilde{X}_N^T]\boldsymbol{\mathcal{I}}_k^T\right), \tag{60}$$

for some dummy variable $\boldsymbol{\Psi}_k^x$, chosen here to be a diagonal matrix. Finally, the constraint in eq. (58) is automatically implied by satisfying the following two constraints as:

$$(\bar{X}_N-\bar{\boldsymbol{\alpha}})^T\boldsymbol{\mathcal{I}}_k^T\boldsymbol{P}_x\boldsymbol{\mathcal{I}}_k(\bar{X}_N-\bar{\boldsymbol{\alpha}})+\mathrm{Tr}(\boldsymbol{\Psi}_k^x)\leq\beta_x, \tag{61}$$

$$\boldsymbol{\Psi}_k^x\succeq\boldsymbol{P}_x\boldsymbol{\mathcal{I}}_k\mathbb{E}[\tilde{X}_N\tilde{X}_N^T]\boldsymbol{\mathcal{I}}_k^T. \tag{62}$$

Thus, eqs. (61) and (62) $\Rightarrow$ eq. (55). Finally, eqs. (61) and (62) can be written as the following LMIs:

$$\begin{bmatrix}\beta_x-\mathrm{Tr}(\boldsymbol{\Psi}_k^x) & (\boldsymbol{\mathcal{A}}_N\mu_0+\boldsymbol{\mathcal{B}}_NV_N-\bar{\boldsymbol{\alpha}})^T\boldsymbol{\mathcal{I}}_k^T\\ (\bullet_{12})^T & \boldsymbol{P}_x^{-1}\end{bmatrix}\succeq 0, \tag{63}$$

$$\begin{bmatrix}\boldsymbol{P}_x^{-1}\boldsymbol{\Psi}_k^x & \boldsymbol{\mathcal{I}}_k\boldsymbol{\mathcal{G}}_1 & \boldsymbol{\mathcal{I}}_k\boldsymbol{\mathcal{G}}_2 & \boldsymbol{\mathcal{I}}_k\boldsymbol{\mathcal{G}}_3 & \boldsymbol{\mathcal{I}}_k\boldsymbol{\mathcal{G}}_4\\ (\bullet_{12})^T & \boldsymbol{\Sigma}_0^{-1} & \mathbf{0} & \mathbf{0} & \mathbf{0}\\ (\bullet_{13})^T & \mathbf{0} & \mathbb{W}_N^{-1} & \mathbf{0} & \mathbf{0}\\ (\bullet_{14})^T & \mathbf{0} & \mathbf{0} & \boldsymbol{\Gamma}_N^a & \mathbf{0}\\ (\bullet_{15})^T & \mathbf{0} & \mathbf{0} & \mathbf{0} & \boldsymbol{\Gamma}_N^s\end{bmatrix}\succeq\mathbf{0}, \tag{64}$$

which has to be satisfied for all $k=0,1,\ldots,N$ along with the LMIs mentioned in theorem 3.1.

V. Convex Constraints on the Control

The feedforward control vector V_N can directly be bounded as a linear convex constraint by bounding every element of the vector $-\bar{\beta}_u\leq V_N\leq\bar{\beta}_u$. However, the bound on the complete control input needs to be carefully written as a convex constraint due to the inverse relation with actuator and sensor precisions. Let us write the constraint on control input at any time k as:

$$\mathbb{E}[\|u_k\|]\leq\beta_u\ \Leftrightarrow\ \mathbb{E}[u_k^Tu_k]\leq\beta_u, \tag{65}$$

$$v_k^Tv_k+\mathbb{E}[\tilde{u}_k^T\tilde{u}_k]\leq\beta_u, \tag{66}$$

for $k=0,1,\cdots,N$, which can also be written in augmented vector form as:

$$V_N^T\boldsymbol{\mathcal{I}}_k^T\boldsymbol{\mathcal{I}}_kV_N+\mathbb{E}[\tilde{U}_N^T\boldsymbol{\mathcal{I}}_k^T\boldsymbol{\mathcal{I}}_k\tilde{U}_N]\leq\beta_u, \tag{67}$$

$$V_N^T\boldsymbol{\mathcal{I}}_k^T\boldsymbol{\mathcal{I}}_kV_N+\mathrm{Tr}\left(\boldsymbol{\mathcal{I}}_k\mathbb{E}[\tilde{U}_N\tilde{U}_N^T]\boldsymbol{\mathcal{I}}_k^T\right)\leq\beta_u. \tag{68}$$

Now, using the same approach as discussed in soft convex state constraints, we can write the soft constraints on control input as:

$$V_N^T\boldsymbol{\mathcal{I}}_k^T\boldsymbol{\mathcal{I}}_kV_N+\mathrm{Tr}(\boldsymbol{\Psi}_k^u)\leq\beta_u,\ \boldsymbol{\Psi}_k^u\succeq\boldsymbol{\mathcal{I}}_k\mathbb{E}[\tilde{U}_N\tilde{U}_N^T]\boldsymbol{\mathcal{I}}_k^T, \tag{69}$$

for some dummy variable Ψ_k^u, which can finally be written as the following LMIs:

$$\begin{bmatrix} \beta_u - \mathrm{Tr}(\Psi_k^u) & V_N^T \mathcal{I}_k^T \\ \mathcal{I}_k V_N & \boldsymbol{I}_m \end{bmatrix} \succeq 0, \tag{70}$$

$$\begin{bmatrix} \Psi_k^u & \mathcal{I}_k \mathcal{H}_1 & \mathcal{I}_k \mathcal{H}_2 & \mathcal{I}_k \mathcal{H}_3 & \mathcal{I}_k \mathcal{H}_4 \\ (\bullet_{12})^T & \Sigma_0^{-1} & \mathbf{0} & \mathbf{0} & \mathbf{0} \\ (\bullet_{13})^T & \mathbf{0} & \mathbb{W}_N^{-1} & \mathbf{0} & \mathbf{0} \\ (\bullet_{14})^T & \mathbf{0} & \mathbf{0} & \Gamma_N^a & \mathbf{0} \\ (\bullet_{15})^T & \mathbf{0} & \mathbf{0} & \mathbf{0} & \Gamma_N^s \end{bmatrix} \succeq \mathbf{0}, \tag{71}$$

which has to be satisfied for all $k = 0, 1, \ldots, N$ along with other constraints required for covariance steering.

VI. Simulation Example

We will use a spacecraft landing problem as an example to find the optimal precision of sensors/actuators for the covariance steering of the lander (see fig. 1). For the assumed lumped mass rigid body model, the translational dynamics is assumed to be decoupled from the attitude dynamics, which is a common assumption as the control capability in translational dynamics is typically of far lower bandwidth than the attitude dynamics [20]. We further assume the mass of the lander to be constant during the landing operation to make the system dynamics linear.

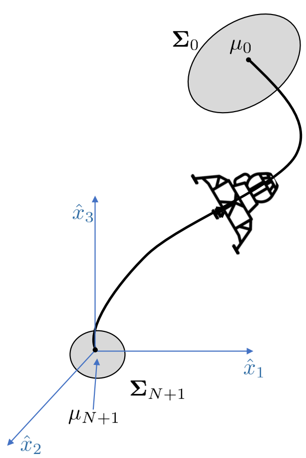

Fig. 1. Soft landing example

The dynamics of the system can be written as [20]:

$$\mathrm{d}x(t) = \boldsymbol{A}(\omega)x(t)\mathrm{d}t + \boldsymbol{B}\left(g\mathrm{d}t + \frac{T(t)\mathrm{d}t + \mathrm{d}w^a}{m}\right), \tag{72}$$

where $x = [x_1 \; x_2 \; x_3 \; \dot{x}_1 \; \dot{x}_2 \; \dot{x}_3]^T \in \mathbb{R}^6$, $g \in \mathbb{R}^3$ is the constant gravity vector, $T \in \mathbb{R}^3$ is the thrust vector and m is the mass of the spacecraft. The constant matrices $\boldsymbol{A}$ and $\boldsymbol{B}$ are defined as:

$$\boldsymbol{A}(\omega) = \begin{bmatrix} \mathbf{0} & \boldsymbol{I} \\ -\boldsymbol{S}(\omega)^2 & -2\boldsymbol{S}(\omega) \end{bmatrix}, \; \boldsymbol{B} = \begin{bmatrix} \mathbf{0} \\ \boldsymbol{I} \end{bmatrix}, \tag{73}$$

with $\boldsymbol{S}(\omega)$ as a skew-symmetric matrix made from the vector $\omega = [\omega_1 \; \omega_2 \; \omega_3] \in \mathbb{R}^3$ representing planet's constant angular velocity vector and the state derivatives defined in the planet surface fixed reference frame. The actuator noise ($w^a(t)$) is modeled as Brownian motion representing uncertainty in the thrusting capabilities of the engine. Now, we discretize the system using zero-order hold (ZOH) approximation to obtain:

$$x_{k+1} = \boldsymbol{A}_k x_k + \boldsymbol{B}_k\left(g + \frac{T_k}{m}\right) + \boldsymbol{D}_k w_k + \boldsymbol{E}_k w_k^a, \tag{74}$$

$$y_k = \boldsymbol{C}_k x_k + \boldsymbol{F}_k w_k^s, \tag{75}$$

where

$$\boldsymbol{A}_k = e^{\boldsymbol{A}\Delta t}, \; \boldsymbol{B}_k = \left(\int_{\tau=0}^{\Delta t} e^{\mathbf{A}\tau} d\tau\right)\mathbf{B}, \tag{76}$$

$$\boldsymbol{D}_k = 0.01\boldsymbol{I}, \; \boldsymbol{E}_k = \frac{\boldsymbol{B}_k}{m}, \; \boldsymbol{C}_k = \boldsymbol{I}, \; \boldsymbol{F}_k = \boldsymbol{I}, \tag{77}$$

where Δt is the sample time and we assume that all the states can be measured with sensor noise (w_k^s) entering through each channel. The disturbance due to process noise (w_k) is directly represented in the discrete equations as a sequence of i.i.d random vectors with covariance $W_p = \boldsymbol{I}$.

The parameters assumed in this example are $g = [0, 0, 3.5]^T$, sample time $\Delta t = 0.2$, mass $m = 1$ kg and number of time-steps $N = 25$. The price values used for actuators and sensors are $p_a = p_s = 0.1$ and the maximum values assumed are $\bar{\gamma}_a = 1e5, \bar{\gamma}_s = 1e5$. YALMIP [21] is used for the numerical implementation of the example. The convex region to bound the states in Fig. 2 is defined using an ellipsoid with $\alpha_x = [0, 0, 9.9, 0, 0, 0]^T$, $\beta_x = 1$ and $\boldsymbol{P}_x = \mathbf{diag}([\frac{1}{25}, \frac{1}{25}, \frac{1}{100}, 0, 0, 0])$ and the convex constraint on control was defined with the parameter $\beta_u = 400$.

Figure 2 shows the simulation result for 100 trajectories while minimizing the cost function J and a budget constraint of $\$10^5$. The mean at final time is chosen as $\mu_{N+1} = [0, 0, 0, 0, 0, 0]^T$ and the covariance as $\Sigma_{N+1} = \mathbf{diag}([.01, .01, .01, .001, .001, 0.001])$ for the case of $\omega = [0, 0, 0]$ rad/sec and same mean with a covariance bound of $\Sigma_{N+1} = \mathbf{diag}([.05, .05, .05, .005, .005, 0.005])$ for the case of $\omega = [0, 0, 1]$ rad/sec. The covariance bound at final time Σ_{N+1} has to be increased to accommodate the case of $\omega_3 = 1$ rad/sec in the same budget constraint (\$).

Figure 3 shows the variation of the scaled covariance (η_Σ) and cost (J) with variation in budget constraint (\$) while minimizing the scaled covariance η_Σ. The scaled covariance (η_Σ) is defined as: $\Sigma_{N+1} = \eta_\Sigma \bar{\Sigma}_{N+1}$ with $\bar{\Sigma}_{N+1} = \mathbf{diag}([.01, .01, .01, .001, .001, 0.001])$. The figure describes that increasing the budget constraint allows for the tighter bound on end-time covariance for

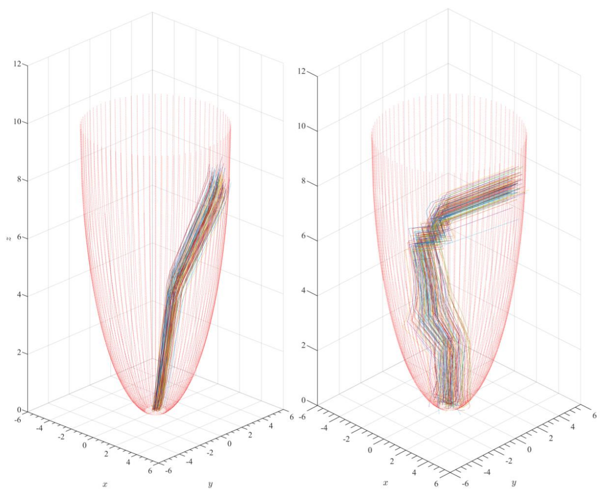

Fig. 2. Powered descent trajectories with optimal precision of sensors and actuators: (left) $\omega = [0, 0, 0]$ rad/sec and (right) $\omega = [0, 0, 1]$ rad/sec.

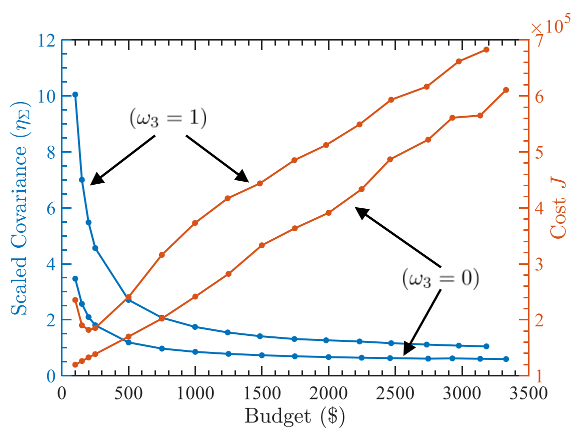

Fig. 3. Scaled covariance (η_Σ) and cost (J) with change in budget limit ($) for two cases of $\omega = [0, 0, 0]$ rad/sec and $\omega = [0, 0, 1]$ rad/sec.

both the cases of $\omega_3 = 0$ rad/sec and $\omega_3 = 1$ rad/sec. Moreover, after around $2000, the scaled covariance (η_Σ) scaled covariance (η_Σ) starts to converge, showing that no considerable improvements can be made in final covariance bound even with higher budget (better sensor/actuator). Also notice that tighter constraint on final-time covariance can be achieved for $\omega_3 = 0$ rad/sec as compared to $\omega_3 = 1$ rad/sec. The cost function J is observed to be monotonically increasing with higher budget for the case of $\omega_3 = 1$ rad/sec. The increase in cost can be understood as higher feedback gain is required to obtain a tighter bound on final-time covariance with increase in budget limit.

Figures 4 and 5 show the variation in actuator precision (γ_a) and sensor precision (γ_s) with the same budget limits as used earlier. Notice that the precision

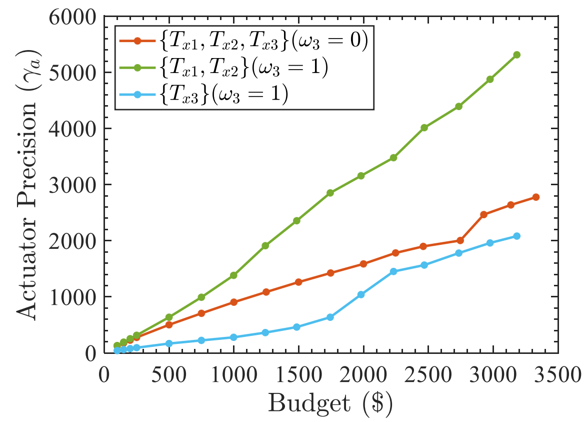

Fig. 4. Optimal actuator precision with change in allowed budget limit $ for two cases of $\omega = [0, 0, 0]$ rad/sec and $\omega = [0, 0, 1]$ rad/sec.

values for both actuators and sensors monotonically increases with an increase in the budget limit. It should also be observed that the actuator precision for the case of $\omega_3 = 1$ rad/sec along $\hat{x}_1$ and $\hat{x}_2$ axis is the same (due to symmetry) and is higher than the precision required along $\hat{x}_3$ axis as shown in Fig. 4. This is due to the rotation of the planet about $\hat{x}_3$ axis that requires more precise thrust in the two perpendicular directions. A similar observation can be made in Fig. 5 with better sensing requirement for both position and velocity along $\hat{x}_1$ and $\hat{x}_2$ axis as compared to $\hat{x}_3$ axis for $\omega_3 = 1$ rad/sec. However, the same sensing requirement is observed along all three directions for $\omega_3 = 0$ rad/sec. For both the cases of $\omega_3 = 0$ rad/sec and $\omega_3 = 1$ rad/sec, it was observed that more precise sensors are required for velocity feedback compared to position feedback.

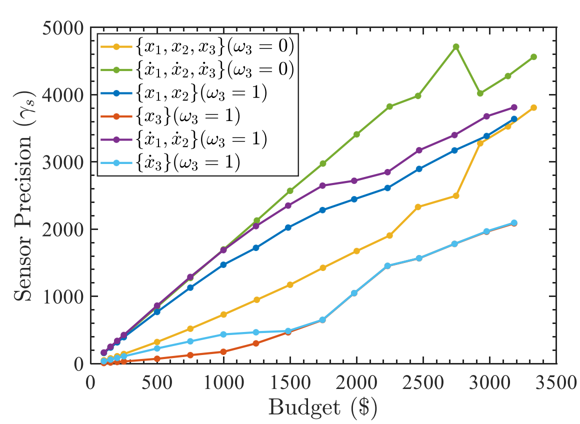

Fig. 5. Optimal sensor precision with change in allowed budget limit $ for two cases of $\omega = [0, 0, 0]$ rad/sec and $\omega = [0, 0, 1]$ rad/sec.

Finally, Fig. 6 shows the simulated powered descent trajectories with a budget constraint of $100 and $3000.

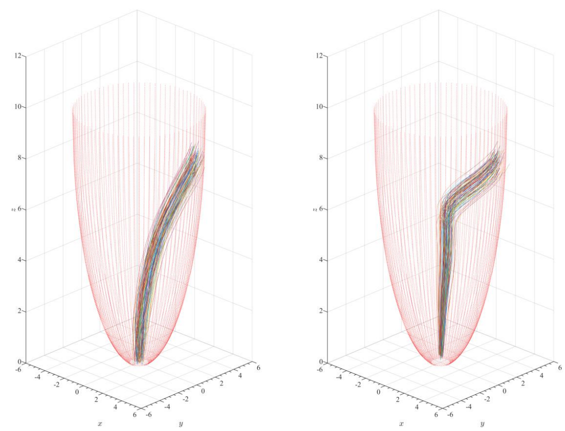

Fig. 6. Powered descent trajectories with optimal precision of sensors and actuators with the budget limit of: (left) \$100 and (right) \$3000 while minimizing the scaled covariance η_Σ.

The important observation here is the difference between the mean path of descent landing trajectories. This is due to a more stringent bound on final-time covariance for the budget limit of \$3000 (see Fig. 3). A higher cost was further observed to achieve the trajectory shown on the right with the budget limit of \$3000, which uses more control effort to push the trajectories towards the center to achieve the stricter covariance bound.

VII. Conclusion

This paper proposed a design strategy for covariance steering using optimal sensor/actuator selection in a finite horizon discrete-time time-varying linear system. The complete problem of designing an affine feedback controller to steer the mean and covariance and simultaneously designing the precision architecture of the system was formulated in the LMI framework. Soft convex constraints on control inputs and states were further added as the expected values to satisfy constraint requirements. A simplified spacecraft landing problem was considered as an example to show the need for hardware design and the performance deterioration with less accurate sensor/actuator precision. The results showed that the best achievable covariance at the final time depends on the precision values of both actuators/sensors which further depends on budget requirement. It was also observed that a saturation limit of achievable state covariance is reached even with increasing budget (sensor/actuator precision) after a certain point.

References

[1] J. Lu and R. E. Skelton. Instrument and control design in linear systems. *International Journal of Control*, 72(9):799–814, 1999.

[2] R. Goyal and R. E. Skelton. Joint optimization of plant, controller, and sensor/actuator design. In *2019 American Control Conference (ACC)*, pages 1507–1512, July 2019.

[3] M. C. De Oliveira and J. C. Geromei. Linear output feedback controller design with joint selection of sensors and actuators. *IEEE Transactions on Automatic Control*, 45(12):2412–2419, Dec 2000.

[4] Raman Goyal and Robert E Skelton. Integrating structure and control design using tensegrity paradigm. In *Advances in Engineering Materials, Structures and Systems: Innovations, Mechanics and Applications*, pages 989–994. CRC Press, 2019.

[5] Siddharth Joshi and Stephen Boyd. Sensor selection via convex optimization. *IEEE Transactions on Signal Processing*, 57(2):451–462, 2009.

[6] Faming Li, Mauricio C. de Oliveira, and Robert E. Skelton. Integrating Information Architecture and Control or Estimation Design. *SICE Journal of Control, Measurement, and System Integration*, Vol.1(No.2), March 2008.

[7] Anthony Hotz and Robert E Skelton. Covariance control theory. *International Journal of Control*, 46(1):13–32, 1987.

[8] R. E Skelton, T. Iwasaki, and K. Grigoriadis. *A Unified Algebraic Approach to Control Design.* Taylor & Francis, London, UK, 1998.

[9] E. Collins and R. Skelton. A theory of state covariance assignment for discrete systems. *IEEE Transactions on Automatic Control*, 32(1):35–41, 1987.

[10] Yongxin Chen, Tryphon T Georgiou, and Michele Pavon. Optimal steering of a linear stochastic system to a final probability distribution, part i. *IEEE Transactions on Automatic Control*, 61(5):1158–1169, 2015.

[11] Yongxin Chen, Tryphon T Georgiou, and Michele Pavon. Optimal steering of a linear stochastic system to a final probability distribution, part ii. *IEEE Transactions on Automatic Control*, 61(5):1170–1180, 2015.

[12] Yongxin Chen, Tryphon T Georgiou, and Michele Pavon. Optimal steering of a linear stochastic system to a final probability distribution—part iii. *IEEE Transactions on Automatic Control*, 63(9):3112–3118, 2018.

[13] Efstathios Bakolas. Finite-horizon covariance control for discrete-time stochastic linear systems subject to input constraints. *Automatica*, 91:61 – 68, 2018.

[14] Efstathios Bakolas. Optimal covariance control for stochastic linear systems subject to integral quadratic state constraints. In *2016 American Control Conference (ACC)*, pages 7231–7236. IEEE, 2016.

[15] Abhishek Halder and Eric DB Wendel. Finite horizon linear quadratic gaussian density regulator with wasserstein terminal cost. In *2016 American Control Conference (ACC)*, pages 7249–7254. IEEE, 2016.

[16] Kazuhide Okamoto and Panagiotis Tsiotras. Optimal stochastic vehicle path planning using covariance steering. *IEEE Robotics and Automation Letters*, 4(3):2276–2281, 2019.

[17] Lars Blackmore, Hui Li, and Brian Williams. A probabilistic approach to optimal robust path planning with obstacles. In *2006 American Control Conference*, pages 7–pp. IEEE, 2006.

[18] Jack Ridderhof and Panagiotis Tsiotras. Minimum-fuel powered descent in the presence of random disturbances. In *AIAA Scitech 2019 Forum*, page 0646, 2019.

[19] Jack Ridderhof, Kazuhide Okamoto, and Panagiotis Tsiotras. Nonlinear uncertainty control with iterative covariance steering. In *2019 IEEE 58th Conference on Decision and Control (CDC)*, pages 3484–3490. IEEE, 2019.

[20] Behçet Açıkmeşe, John M Carson, and Lars Blackmore. Lossless convexification of nonconvex control bound and pointing constraints of the soft landing optimal control problem. *IEEE Transactions on Control Systems Technology*, 21(6):2104–2113, 2013.

[21] Johan Lofberg. Yalmip: A toolbox for modeling and optimization in matlab. In *2004 IEEE international conference on robotics and automation (IEEE Cat. No. 04CH37508)*, pages 284–289. IEEE, 2004.